PROCEEDINGS OF SCIENCE

VERITAS Observations of MGRO J1908+06

Tobias Kleiner[a,b,*] **for the VERITAS collaboration**

[a] *Desy Zeuthen,*
Platanenallee 6, 15738 Zeuthen, Germany
[b] *Humboldt-Universität zu Berlin, Math. - Nat. Fakultät,*
Rudower Chaussee 25, 12489 Berlin, Germany

E-mail: tobias.kleiner@desy.de

MGRO J1908+06 is an extended and powerful source of gamma-ray emission located at (lon= 40.39, lat= −0.79). It was first detected by the Milagro observatory in a northern galactic plane survey in 2007 [1]. It has been the subject of numerous studies in an effort to understand the origin of its gamma-ray emission. Several potential counterparts have been suggested, including the supernova remnant G40.5-0.5 and the pulsar J1907+0602 [2]. The observed Tera-electronvolt emission may originate from interactions between the pulsar wind nebula and molecular clouds or the supernova remnant shell. However, the question of the true nature of the source remains open, mainly due to the existence of multiple potential counterparts. Recent observations of emission exceeding several hundred TeV [3] make MGRO J1908+06 a strong contender for a Pevatron — a source with the ability to accelerate particles to Peta-electronvolt energies. The detected emission at such high energies indicates the presence of an extremely powerful and efficient particle acceleration mechanism within this source. Over a span of more than 10 years, the MGRO J1908+06 region has been observed by VERITAS for approximately 130h. This allows to study the energy dependent morphology of the source and a leptonic origin of the gamma-ray emission is investigated.

38th International Cosmic Ray Conference (ICRC2023)
26 July - 3 August, 2023
Nagoya, Japan

*Speaker

PoS(ICRC2023)762

1. Introduction

The VERITAS air Cherenkov telescope array is located at the Fred Lawrence Whipple Observatory (FLWO) in southern Arizona (31 40N, 110 57W, 1.3km a.s.l.). VERITAS observes gamma-ray sources over the energy range from 100 GeV to >30 TeV with an energy resolution of 15-25 %, angular resolution of $< 0.1^\circ$ (68 %) at 1 TeV and detects a point source with 1 % of the flux of the Crab Nebula within 25 h. MGRO J1908+06 was first detected by the Milagro observatory in the VHE range (300 GeV - 20 TeV) in a northern galactic plane survey in 2007 [1] and subsequently confirmed by other observatories such as H.E.S.S. [4], VERITAS [5], ARGO-YBJ [6], HAWC [7], and LHAASO [3].

2. Observation and Analysis

VERITAS observed the MGRO J1908+06 region for more than a decade. The analysis presented here incorporates observations taken between 2009 and 2022 with a total livetime of approximately 130 h. The analysis uses updated 3D maximum likelihood methods together with the FoVbackground estimation technique, relying on novel 3D VERITAS background models, that take into account changes in observing conditions and upgrades to the instrument [8]. The background models describe the background rate as a function of FoV camera coordinate and energy. MGRO J1908+06 is a strong and extended source located approximately 1° from the western jet lobe of SS 433. The MGRO J1908+06 region has been measured to harbour largely extended emission at TeV energies and is populated with several gamma-ray sources. Hence, exclusion regions are placed to assure that the background model is fit only to regions devoid of gamma-ray signal: a 1.5° exclusion region around 3HWC J1908+063 and 0.5° exclusion regions for the pulsars J1907+0602, J1906+0722, SNRs G40.5-0.5, G41.1-0.3, and the eastern and western emission hotspots of SS 433 (e1,e2), (w1,w2). In order to evaluate and address systematic effects, five independent "mimic" datasets are generated that closely replicate the observation conditions of the MGRO J1908+06 dataset in terms of azimuth, zenith angle, night-sky background rate, exposure, and VERITAS instrument status. These mimic datasets are derived from actual VERITAS observations of gamma-ray-free regions, by changing the pointing to a new derived pointing at the region of MGRO J1908+06. Each mimic observation is selected and transformed based on the distribution of observation conditions in the MGRO J1908+06 dataset. This means that the mimic observations are modified on a run-per-run basis, adjusting the event list and pointing information according to the computed mimic pointings. The mimic observations are then processed alongside the actual MGRO J1908+06 observations using the VERITAS low-level analysis tool Eventdisplay. Gamma-hadron separation cuts are used, which are optimized for sources with hard spectral indices of ~ 2. The MGRO J1908+06 dataset is corrected by the average excess bias obtained from the five mimic datasets, which match the observation conditions of the MGRO J1908+06 observations. Comparing the flux between the uncorrected and corrected datasets, it can be inferred that the influence of the large exclusion mask on the absolute change in flux is minimal. The systematic error, determined as the RMS of the flux from the five mimic datasets (see table 1), is in the range of $5-12$ % in the selected energy ranges. Taking into account statistical errors and the systematic flux error estimate of 25 % for VERITAS, the total uncertainty for the flux points can be estimated

Dataset	**Differential flux (1 / (TeV cm^2 s))**			
	Energy range (GeV)			
	794 - 1580	1580 - 3160	3160 - 6310	6310 - 12600
m.1	3.37e-13	2.33e-13	1.14e-14	-11.1e-15
m.2	-4.55e-13	0.12e-13	1.71e-14	-3.48e-15
m.3	4.03e-13	1.47e-13	6.17e-14	-6.37e-15
m.4	-2.40e-13	4.00e-13	3.30e-14	6.10e-15
m.5	-4.14e-13	-1.03e-13	-2.65e-14	-3.41e-15
RMS	3.77e-13	3.21e-13	3.47e-14	6.68e-15
On	8.13e-12	1.70e-12	3.60e-13	5.66e-14
On$_{red}$	7.17e-12	1.78e-12	3.69e-13	5.7e-14

Table 1: Differential flux values from the five independent mimic datasets (m.1 - m.5) and their RMS error in five bins in energy together with the flux values for the initial MGRO J1908+06 observations and the bias corrected flux values On$_{red}$ for MGRO J1908+06.

Type	**Parameter**	**Value**	**Unit**	**Error**
spectral	Γ	2.34		0.05
	ϕ_0	9.96e-12	cm-2 s-1 TeV-1	6.10e-13
	E_0	1.0	TeV	fixed
spatial	lon	286.97	deg	0.02
	lat	6.39	deg	0.02
	σ	0.46	deg	0.02

Table 2: Best fit parameters from a symmetric Gaussian spatial and a power-law spectral model in the energy range between 0.8 TeV to 12.3 TeV for the MGRO J1908+06 gamma-ray emission.

between 26 % to 30 %. Figure 1 shows the resulting significance map after bias correction. The highest significance is seen at the PSR J1907+0602 and around the 3HAWC J1908+063 position. The VERITAS flux points of MGRO J1908+06 with statistical and systematic uncertainties are given in figure 2 along with the flux points by *Fermi-LAT*, H.E.S.S., HAWC and LHAASO. The results have been cross checked by an independent VERITAS analysis optimized for the analysis of extended sources [9]. The gamma-ray flux measured by VERITAS is in good agreement with the values reported by H.E.S.S., HAWC and LHAASO [3, 10, 11].

The morphological properties of the MGRO J1908+06 source are determined in a 3D maximum-likelihood analysis with a power-law spectral model and a Gaussian spatial model. The best-fit parameters are given in table 2. The best-fit spectral index is 2.34 ± 0.05 in the energy range between 0.8 TeV to 12.6 TeV and an extension of 0.46° is obtained. The significance of the Gaussian model versus the null hypothesis is 34.5 σ, indicating a clear detection and a substantial increase in significance compared to the previous VERITAS analysis, which resulted in a detection with 14 σ. To investigate if the energy dependent morphology of MGRO J1908+06 can be modelled with individual components, the spectromorphological models are fit to the dataset in two slices in

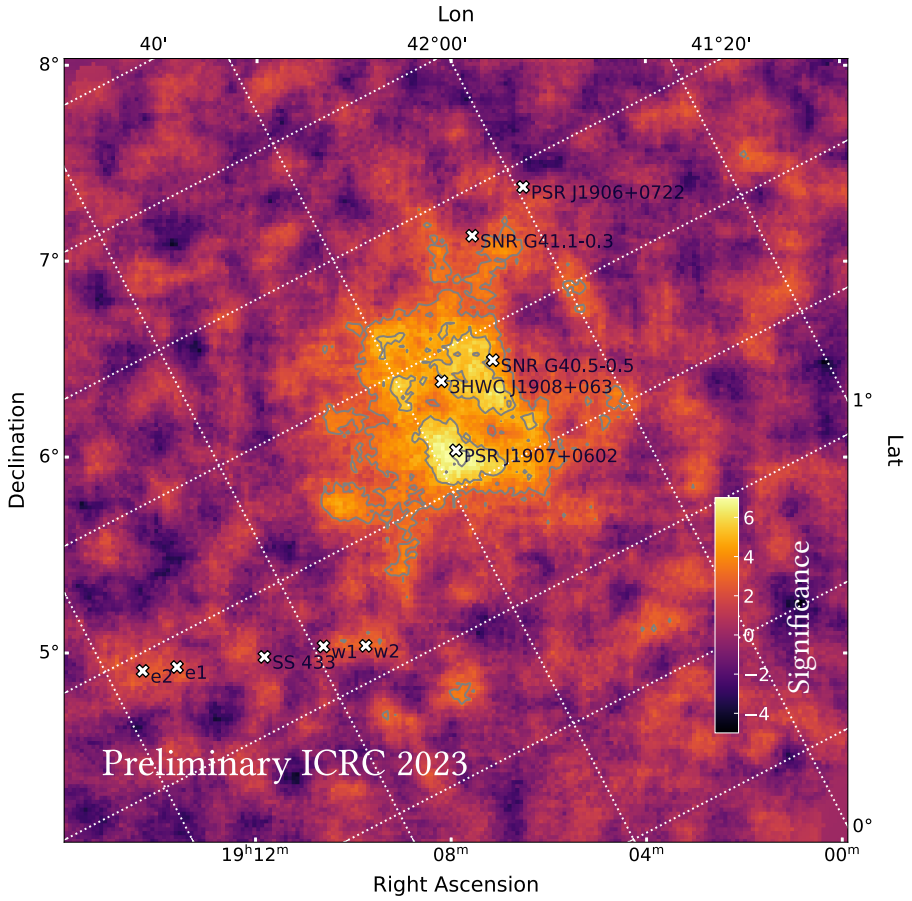

Figure 1: Significance map of the MGRO J1908+06 region after bias correction. The contours indicate the significance values of 3, 5 and 7 σ. Possible associated sources are indicated with white crosses: The SNR G40.5-0.5, SNR G41.1-0.3, PSR J1907+0602 and PSR J1906+0722.

energy, from 0.8 TeV to 3.05 TeV and 3.05 TeV to 12.3 TeV.

The best fit results are displayed in table 3. The results indicate that the centroid position of the Gaussian moves closer to the pulsar location in the selected high energy slice. The separation between the centroid of both models amounts to $0.15 \pm 0.05\,^{\circ}$. This is largely exceeding the systematic uncertainties associated with the pointing accuracy of VERITAS, which is estimated at 20 arc-seconds [13]. It is also larger than the VERITAS gamma-ray point spread function, which is $< 0.1^{\circ}$ at the position of MGRO J1908+06 in this analysis. There is no noticeable difference between the extension of the Gaussian models at the two energy ranges. However, a softening of the spectral index towards higher energies is observed.

To investigate leptonic and hadronic emission scenarios, an analysis of the molecular clouds at the location of the gamma-ray emission is performed. Figure 3 depicts the velocity-integrated column densities in ^{12}CO, obtained from the archive of the 1.2 m CO survey data-verse of the Smithsonian Astrophysical Observatory [14]. The integrated column density maps correspond to two distance ranges: 0.7 to 2.5 kpc (corresponding to a velocity range of 10 to 40 km s^{-1}) and 2.5 to 4.8 kpc (corresponding to a velocity range of 40 to 70 km s^{-1}). The map indicates, that the bulk of

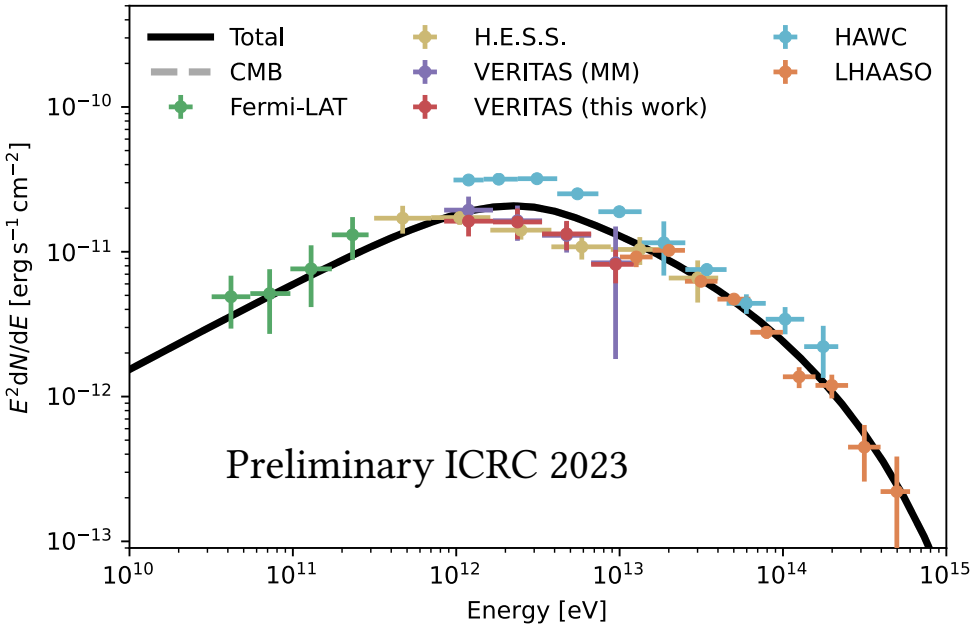

Figure 2: Multi-wavelength spectral energy distribution of MGRO J1908+06 (centered at the PSR J1907+06 location) emission region. The flux points are from *Fermi*-LAT [12], H.E.S.S. [10], HAWC [11] and LHAASO [3]. The results from this work are consistent with the matrix method (MM) results [9]. The flux points are fit with a leptonic model consisting of a synchrotron and inverse Compton component. The primary electron spectrum is described by an exponential cut-off broken power-law spectrum.

Energy range	**Right ascension**	**Declination**	**Extension**	**Γ**	$\boldsymbol{\phi_0}$
(TeV)	**(deg)**	**(deg)**	**1 σ (deg)**		**1/(cm^{2}sTeV)**
0.80 – 3.05	286.98 ± 0.03	6.44 ± 0.03	0.47 ± 0.02	2.19 ± 0.12	$(9.61 \pm 0.74) \cdot 10^{-12}$
3.05 – 12.3	286.95 ± 0.04	6.28 ± 0.04	0.48 ± 0.03	2.63 ± 0.20	$(1.58 \pm 0.51) \cdot 10^{-11}$

Table 3: Spectromorphological fit results in two bins in energy with a Gaussian spatial and a power-law spectral model with spectral index Γ and amplitude ϕ_o at $E_{\rm ref}$ = 1 TeV.

the gamma-ray emission lies in a cavity of low molecular cloud density, from which can be inferred that a leptonic origin of the gamma-ray emission is more likely.

Based on the analysis of the CO data and the proximity of the emission above the break energy to the PSR J1907+0602, a leptonic emission scenario is considered in the following. The multi-wavelength spectral energy distribution fit is performed with the Naima package [15]. An exponential cut-off broken power-law particle distribution is used to describe the electron population. The model for the multi-wavelength spectrum contains a synchrotron component and IC scattering on soft photons from the CMB. No further seed photon fields are included due to the assumed age of the pulsar. The parameters of the model are estimated using MCMC sampling [16]. The result of the fit to XMM-Newton, *Fermi*-LAT, H.E.S.S., VERITAS, HAWC and LHAASO observations is displayed in figure 2. The best-fit results are given in table 4.

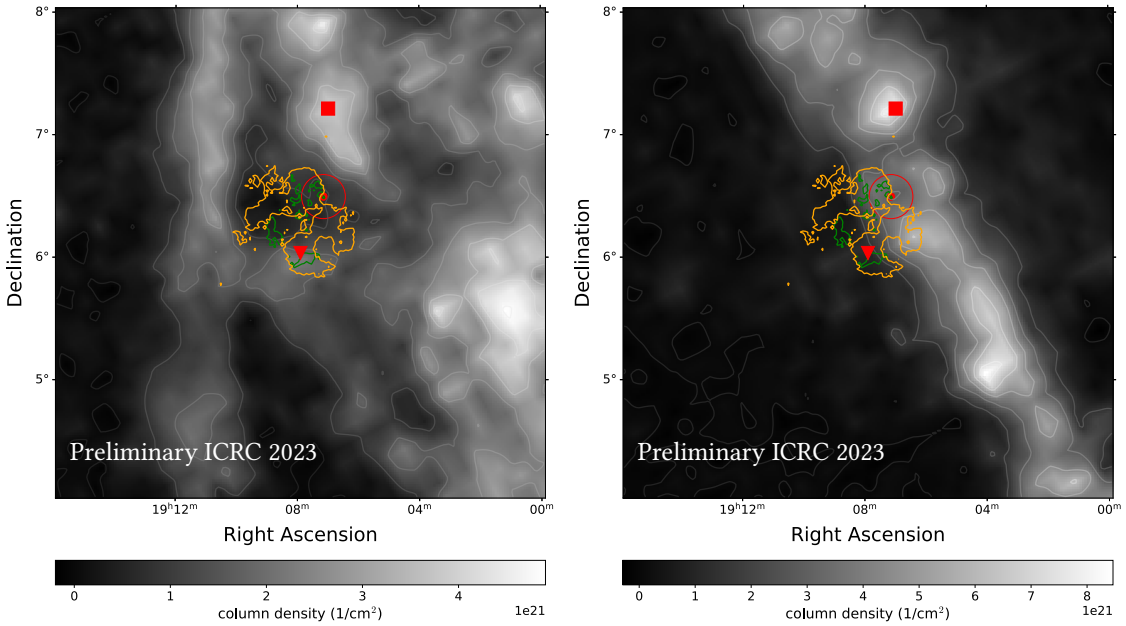

Figure 3: Column density map in ^{12}CO (J=1-0) in the velocity range between (left) [10, 40] km/s and (right) [40, 70] km/s. The contours indicate the gamma-ray morphology 5σ significance level in the energy of [0.8, 3.05] TeV (VERITAS, green contour, this work), and [3.05, 12.3] TeV (VERITAS, orange contour, this work). Three possible counterparts are marked: The PSR 1907+0602 (triangle), SNR G40.5-05 (dot-circle, circle radius according to SNR extension of 0.18°) and *Fermi*-LAT 4FGL source PSR J1906.9+0712 (square).

A	α_1	α_2	E_{break}	E_{cutoff}	B
1/eV			TeV	TeV	μG
$4.00^{+4}_{-2} \cdot 10^{34}$	$1.8^{+0.3}_{-0.5}$	$3.36^{+0.11}_{-0.15}$	19.19 ± 3	800^{+4000}_{-400}	5^{+5}_{-4}

Table 4: Best-fit parameters of the model for the electron injection spectrum fit to the multi-wavelength spectrum of MGRO J1908+06. The parameters are the amplitude A (in particles per unit energy, i.e. 1/eV), the break energy $E_{\rm break}$, the indices α_1 (α_2) for the electron power-law index before (after) the energy break and the exponential cut-off energy $E_{\rm cutoff}$.

3. Conclusion and Discussion

A scenario is considered where the PSR J1907+0602 is moving from the central part of MGRO J1908+06 to its current position. The pulsar was previously detected and its characteristic age was estimated at 19.5 kyr [17]. Furthermore, X-ray observations of PSR J1907+0602 revealed hints of a bow shock in front of the pulsar, resulting from its movement through the interstellar medium [18]. The energy-dependent analysis of MGRO J1908+06 revealed a shift in the emission towards the current position of the pulsar at higher energies. Additionally, a molecular cloud cavity was observed, indicating the remnants of a supernova explosion that gave rise to the PWN observed by Fermi-LAT, HAWC, and VERITAS. Evidence of synchrotron cooling was also detected, with a break in the electron and photon spectra. As a result, electrons from recent times are concentrated around the current PSR location, while earlier injected electrons have cooled down and are located

closer to the previous pulsar position. This suggests that the pulsar J1907+0602 has moved to its current position over its lifetime. The displacement of the pulsar can be attributed to a kick imparted by the supernova explosion, which left behind the pulsar J1907+0602. As a consequence, two distinct PWNe are formed: a relic PWN at the previous location and a new PWN at the current position. Proper motion measurements of the PSR J1908+06 are needed to further support this scenario. Furthermore, a hadronic contribution can not be completely ruled out due to several potential hadronic sources present in the region. Notably, the 4FGL source 1906.9+0712, which is marked by a red square in figure 3, has been identified as a potential site of proton acceleration.

4. Acknowledgements

"This research is supported by grants from the U.S. Department of Energy Office of Science, the U.S. National Science Foundation and the Smithsonian Institution, by NSERC in Canada, and by the Helmholtz Association in Germany. This research used resources provided by the Open Science Grid, which is supported by the National Science Foundation and the U.S. Department of Energy's Office of Science, and resources of the National Energy Research Scientific Computing Center (NERSC), a U.S. Department of Energy Office of Science User Facility operated under Contract No. DE-AC02-05CH11231. We acknowledge the excellent work of the technical support staff at the Fred Lawrence Whipple Observatory and at the collaborating institutions in the construction and operation of the instrument."

This research made use of gammapy,[1] a community-developed core Python package for TeV gamma-ray astronomy [19]. This research made use of Naima [15].

References

[1] A.A. Abdo, B. Allen, D. Berley, S. Casanova, C. Chen, D.G. Coyne et al., *TeV Gamma-Ray Sources from a Survey of the Galactic Plane with Milagro*, *The Astrophysical Journal* **664** (2007) L91.

[2] E. Aliu, S. Archambault, T. Aune, B. Behera, M. Beilicke, W. Benbow et al., *INVESTIGATING THE TeV MORPHOLOGY OF MGRO J1908+06 WITH VERITAS*, *The Astrophysical Journal* **787** (2014) 166.

[3] Z. Cao, F.A. Aharonian, Q. An, Axikegu, L.X. Bai, Y.X. Bai et al., *Ultrahigh-energy photons up to 1.4 petaelectronvolts from 12 γ-ray Galactic sources*, *Nature* **594** (2021) 33.

[4] F. Aharonian, A.G. Akhperjanian, G. Anton, U.B.d. Almeida, A.R. Bazer-Bachi, Y. Becherini et al., *Detection of very high energy radiation from HESS J1908+063 confirms the Milagro unidentified source MGRO J1908+06*, *Astronomy & Astrophysics* **499** (2009) 723.

[5] J.E. Ward, *VERITAS Observations of Mgro J1908+06/Hess J1908+063*, in *AIP Conference Proceedings*, pp. 301–303, 2008, DOI.

[1] https://www.gammapy.org

[6] B. Bartoli, P. Bernardini, X.J. Bi, C. Bleve, I. Bolognino, P. Branchini et al., *OBSERVATION OF THE TeV GAMMA-RAY SOURCE MGRO J1908+06 WITH ARGO-YBJ*, *The Astrophysical Journal* **760** (2012) 110.

[7] A.U. Abeysekara, A. Albert, R. Alfaro, C. Alvarez, J.D. Álvarez, R. Arceo et al., *The 2HWC HAWC Observatory Gamma-Ray Catalog*, *The Astrophysical Journal* **843** (2017) 40.

[8] L. Mohrmann, A. Specovius, D. Tiziani, S. Funk, D. Malyshev, K. Nakashima et al., *Validation of open-source science tools and background model construction in -ray astronomy*, .

[9] V. VERITAS Collaboration, *preliminary results; private communication*, 2023.

[10] D. Kostunin, L. Mohrmann, E.d.O. Wilhelmi, V. Joshi, A. Mitchell, S. Ohm et al., *Revisiting the PeVatron candidate MGRO J1908+06 with an updated H.E.S.S. analysis*, in *Proceedings of 37th International Cosmic Ray Conference — PoS(ICRC2021)*, p. 779, July, 2021, DOI.

[11] A. Albert, R. Alfaro, C. Alvarez, J.D. Álvarez, J.R.A. Camacho, J.C. Arteaga-Velázquez et al., *HAWC Study of the Ultra-high-energy Spectrum of MGRO J1908+06*, *The Astrophysical Journal* **928** (2022) 116.

[12] J. Li, R.-Y. Liu, E.d.O. Wilhelmi, D.F. Torres, Q.-C. Liu, M. Kerr et al., *Investigating the Nature of MGRO J1908+06 with Multiwavelength Observations*, *The Astrophysical Journal Letters* **913** (2021) L33.

[13] C.B. Adams, W. Benbow, A. Brill, J.H. Buckley, J.L. Christiansen, A. Falcone et al., *The throughput calibration of the VERITAS telescopes*, *Astronomy & Astrophysics* **658** (2022) A83.

[14] T.M. Dame, D. Hartmann and P. Thaddeus, *DHT08_quad1_interp.fits*, 2011. 10.7910/DVN/1PG9NV/SR7YUB.

[15] V. Zabalza, *Naima: a Python package for inference of particle distribution properties from nonthermal spectra*, .

[16] D. Foreman-Mackey, D.W. Hogg, D. Lang and J. Goodman, *emcee: The MCMC Hammer*, *Publications of the Astronomical Society of the Pacific* **125** (2013) 306.

[17] A.A. Abdo, M. Ackermann, M. Ajello, L. Baldini, J. Ballet, G. Barbiellini et al., *PSR J1907+0602: A RADIO-FAINT GAMMA-RAY PULSAR POWERING A BRIGHT TeV PULSAR WIND NEBULA*, *The Astrophysical Journal* **711** (2010) 64.

[18] D. Pandel and R. Scott, *Multi-wavelength studies of the gamma-ray pulsar PSR J1907+0602*, pp. 329–332, 2012, DOI.

[19] C. Deil, R. Zanin, J. Lefaucheur, C. Boisson, B. Khélifi, R. Terrier et al., *Gammapy - A prototype for the CTA science tools*, Sept., 2017. 10.48550/arXiv.1709.01751.

Full Author List: VERITAS Collaboration

A. Acharyya[1], C. B. Adams[2], A. Archer[3], P. Bangale[4], J. T. Bartkoske[5], P. Batista[6], W. Benbow[7], J. L. Christiansen[8], A. J. Chromey[7], A. Duerr[5], M. Errando[9], Q. Feng[7], G. M. Foote[4], L. Fortson[10], A. Furniss[11,12], W. Hanlon[7], O. Hervet[12], C. E. Hinrichs[7,13], J. Hoang[12], J. Holder[4], Z. Hughes[9], T. B. Humensky[14,15], W. Jin[1], M. N. Johnson[12], M. Kertzman[3], M. Kherlakian[6], D. Kieda[5], T. K. Kleiner[6], N. Korzoun[4], S. Kumar[14], M. J. Lang[16], M. Lundy[17], G. Maier[6], C. E McGrath[18], M. J. Millard[19], C. L. Mooney[4], P. Moriarty[16], R. Mukherjee[20], S. O'Brien[17,21], R. A. Ong[22], N. Park[23], C. Poggemann[8], M. Pohl[24,6], E. Pueschel[6], J. Quinn[18], P. L. Rabinowitz[9], K. Ragan[17], P. T. Reynolds[25], D. Ribeiro[10], E. Roache[7], J. L. Ryan[22], I. Sadeh[6], L. Saha[7], M. Santander[1], G. H. Sembroski[26], R. Shang[20], M. Splettstoesser[12], A. K. Talluri[10], J. V. Tucci[27], V. V. Vassiliev[22], A. Weinstein[28], D. A. Williams[12], S. L. Wong[17], and J. Woo[29]

[1]Department of Physics and Astronomy, University of Alabama, Tuscaloosa, AL 35487, USA
[2]Physics Department, Columbia University, New York, NY 10027, USA
[3]Department of Physics and Astronomy, DePauw University, Greencastle, IN 46135-0037, USA
[4]Department of Physics and Astronomy and the Bartol Research Institute, University of Delaware, Newark, DE 19716, USA
[5]Department of Physics and Astronomy, University of Utah, Salt Lake City, UT 84112, USA
[6]DESY, Platanenallee 6, 15738 Zeuthen, Germany
[7]Center for Astrophysics | Harvard & Smithsonian, Cambridge, MA 02138, USA
[8]Physics Department, California Polytechnic State University, San Luis Obispo, CA 94307, USA
[9]Department of Physics, Washington University, St. Louis, MO 63130, USA
[10]School of Physics and Astronomy, University of Minnesota, Minneapolis, MN 55455, USA
[11]Department of Physics, California State University - East Bay, Hayward, CA 94542, USA
[12]Santa Cruz Institute for Particle Physics and Department of Physics, University of California, Santa Cruz, CA 95064, USA
[13]Department of Physics and Astronomy, Dartmouth College, 6127 Wilder Laboratory, Hanover, NH 03755 USA
[14]Department of Physics, University of Maryland, College Park, MD, USA
[15]NASA GSFC, Greenbelt, MD 20771, USA
[16]School of Natural Sciences, University of Galway, University Road, Galway, H91 TK33, Ireland
[17]Physics Department, McGill University, Montreal, QC H3A 2T8, Canada
[18]School of Physics, University College Dublin, Belfield, Dublin 4, Ireland
[19]Department of Physics and Astronomy, University of Iowa, Van Allen Hall, Iowa City, IA 52242, USA
[20]Department of Physics and Astronomy, Barnard College, Columbia University, NY 10027, USA
[21] Arthur B. McDonald Canadian Astroparticle Physics Research Institute, 64 Bader Lane, Queen's University, Kingston, ON Canada, K7L 3N6
[22]Department of Physics and Astronomy, University of California, Los Angeles, CA 90095, USA
[23]Department of Physics, Engineering Physics and Astronomy, Queen's University, Kingston, ON K7L 3N6, Canada
[24]Institute of Physics and Astronomy, University of Potsdam, 14476 Potsdam-Golm, Germany
[25]Department of Physical Sciences, Munster Technological University, Bishopstown, Cork, T12 P928, Ireland
[26]Department of Physics and Astronomy, Purdue University, West Lafayette, IN 47907, USA
[27]Department of Physics, Indiana University-Purdue University Indianapolis, Indianapolis, IN 46202, USA
[28]Department of Physics and Astronomy, Iowa State University, Ames, IA 50011, USA
[29]Columbia Astrophysics Laboratory, Columbia University, New York, NY 10027, USA

PoS(ICRC2023)762